

Ground-state properties of the $S=1/2$ Heisenberg antiferromagnet on a triangular lattice: a numerical study of a finite cell

This article has been downloaded from IOPscience. Please scroll down to see the full text article.

1990 J. Phys. A: Math. Gen. 23 L1043

(<http://iopscience.iop.org/0305-4470/23/19/005>)

View [the table of contents for this issue](#), or go to the [journal homepage](#) for more

Download details:

IP Address: 129.252.86.83

The article was downloaded on 01/06/2010 at 08:58

Please note that [terms and conditions apply](#).

LETTER TO THE EDITOR

Ground-state properties of the $S = \frac{1}{2}$ Heisenberg antiferromagnet on a triangular lattice: a numerical study of a finite cell

R Deutscher[†], H U Everts[†], S Miyashita^{†‡} and M Wintel[†]

[†] Institut für Theoretische Physik, Universität Hannover, Appelstr. 2, D-3000 Hannover 1, Federal Republic of Germany

[‡] Kyoto University, Department of Physics, College of Liberal Arts and Sciences, Kyoto 606, Japan

Received 30 July 1990

Abstract. We study numerically a 21-site Marland-Betts type cell of the $S = \frac{1}{2}$ Heisenberg antiferromagnet on a triangular lattice with nearest-neighbour (NN) and next-nearest-neighbour (NNN) couplings. The emphasis is on a comparison of the classical picture of this model with its quantum properties. By considering the structure function $S(\mathbf{k})$ we demonstrate that there is a close connection between the classical and the quantum ground states of the system. Contrary to a previous conjecture we find no significant enhancement of the chiral order parameter with increasing strength of the NNN coupling.

Two-dimensional antiferromagnetic spin- $\frac{1}{2}$ Heisenberg models have played an important role in the discussion of the properties of strongly correlated electron systems in two dimensions. Anderson conjectured [1] that the ground state of such electron systems should be similar to the resonating valence bond (RVB) state which he had previously proposed as the ground state of the antiferromagnetic spin- $\frac{1}{2}$ Heisenberg model on the triangular lattice [2]. The frustrating interactions of the triangular antiferromagnet were thought to destroy the long-ranged Néel order which appears to prevail on the unfrustrated square lattice [3] and to favour the disordered RVB state. Recent numerical studies [4] as well as variational and semiclassical analyses [5] of frustrated Heisenberg models have, however, cast doubts on this simple picture. In wide regions of the parameter spaces of these models their ground states seem to be ordered states which are reminiscent of the spin structures that emerge in the classical approach. It has however also been shown that for triangular antiferromagnets the nearest-neighbour (NN) interactions can be supplemented by next-nearest-neighbour (NNN) interactions and by four-spin couplings such that they possess an RVB state as their ground state [6]. More exotic RVB-like states that break time reversal invariance and parity have also been suggested as ground states of frustrated Heisenberg models [7]. In particular, it has been argued that for these states the pseudoscalar variable $\chi_{ijk} = \mathbf{S}_i \cdot (\mathbf{S}_j \times \mathbf{S}_k)$ defined on an elementary triangular plaquette with corners i, j, k should have a uniform extensive expectation value [8]. A numerical study of the triangular Heisenberg antiferromagnet with NN interaction only has not yielded evidence for this chiral symmetry breaking [9]. According to [8] this was not to be expected as chiral symmetry breaking should only occur when the NNN interaction exceeds a critical value.

In this letter we present the results of a numerical diagonalization of the antiferromagnetic Heisenberg model with NN and NNN interaction on a triangular lattice,

$$H = 2J \left(\sum_{\text{NN}} \mathbf{S}_i \cdot \mathbf{S}_j + \alpha \sum_{\text{NNN}} \mathbf{S}_i \cdot \mathbf{S}_j \right) \quad (1)$$

where \mathbf{S}_i denote the spin- $\frac{1}{2}$ matrices at the lattice site \mathbf{R}_i .

The numerical diagonalization was performed for a 21-site Marland-Betts type cell [10] with periodic boundary conditions.

Jolicœur *et al* [11] have recently studied the ground state properties of (1) by means of the spin wave approximation and by a numerical analysis of a 12-site cell. As their main result they find that the ground state of the model breaks the lattice rotational invariance spontaneously, when the NNN coupling α exceeds a critical value. In this letter we also address the question of how the structure of the ground state of (1) changes when the parameter α is varied, but we focus our attention on the role of the wavevectors in the quantum and the classical description of the system.

The main aim of the present letter is to point out the connections between the quantum states and the classical spin configurations of the model (1). As will be seen, these connections are most clearly reflected by the structure function $S(\mathbf{k})$ which we have determined numerically. We shall also present results for the chiral order parameter of the 21-site system.

At first we have to briefly review the classical treatment of the Hamiltonian (1) in which the spin operators \mathbf{S}_i are considered as classical vectors \mathbf{S}_i . The Hamiltonian is then diagonalized by introducing the Fourier transforms

$$\mathbf{S}_q = (1/\sqrt{N}) \sum_i \mathbf{S}_i e^{iq \cdot \mathbf{R}_i}. \quad (2)$$

This yields

$$H = 2 \sum_q J(\mathbf{q}) \mathbf{S}_q \cdot \mathbf{S}_{-\mathbf{q}} \quad (3)$$

where

$$J(\mathbf{q}) = \cos(q_x) + 2 \cos(q_x/2) \cos(\sqrt{3} q_y/2) + \alpha (\cos(\sqrt{3} q_y) + 2 \cos(3q_x/2) \cos(\sqrt{3} q_y/2)) \quad (4)$$

is the Fourier transform of the exchange couplings of (1) (here and in the following we set $J = 1$). Generically, the classical ground states are planar spiral spin configurations [12],

$$\mathbf{S}_i = \mathbf{e}_1 \cos(\mathbf{k} \cdot \mathbf{R}_i) + \mathbf{e}_2 \sin(\mathbf{k} \cdot \mathbf{R}_i) \quad (5)$$

where $\mathbf{e}_1, \mathbf{e}_2$ are an arbitrary pair of orthogonal unit vectors. For a given value of α the wavevector \mathbf{k} of the spiral is that vector within the first Brillouin zone (BZ) that minimizes $J(\mathbf{q})$, and the corresponding energy per site is

$$E^{\text{cl}}(\mathbf{k}) = 2J(\mathbf{k}). \quad (6)$$

From (4) one easily finds the following results [11].

(i) For $0 < \alpha < \frac{1}{3}$, $J(\mathbf{k})$ is minimal at the corners of the hexagonal BZ of the triangular lattice figure 1. Only two of these points, e.g., $\mathbf{k}_1 = \pi \cdot (\frac{4}{3}, 0)$ and $-\mathbf{k}_1$ are independent, the others being connected to them by reciprocal lattice vectors. The corresponding spin configurations are the two 120 degree spiral structures which differ by their helicity. The classical energy is $E^{\text{cl}}(\mathbf{k}_1) = 3(2\alpha - 1)$.

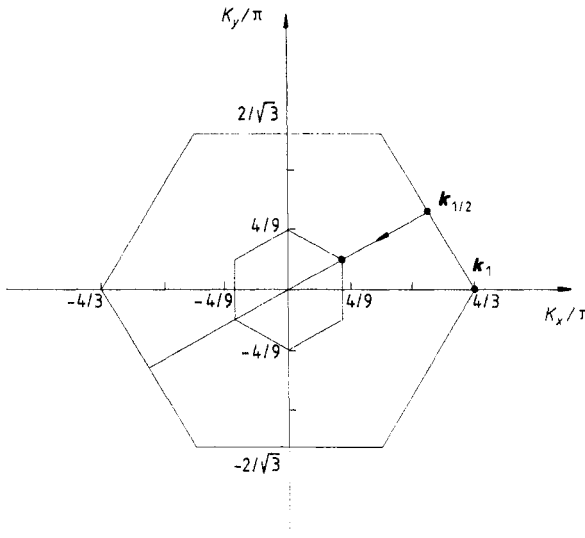


Figure 1. Path of a minimum of $J(\mathbf{q})$ within the Brillouin zone of the triangular lattice when α is varied. The small hexagon inside is the Brillouin zone of one of the sublattices.

(ii) For $\frac{1}{8} < \alpha < 1$ new global minima develop at $\mathbf{k}_{1/2} = \pi \cdot (1, 1/\sqrt{3})$ and at the five equivalent points bisecting the faces of the BZ so that the ground state changes discontinuously at $\alpha = \frac{1}{8}$. $\mathbf{k}_{1/2}$ is half a reciprocal lattice vector. This is one of the special situations first discussed by Villain [13] where in addition to the spiral ground state (4) with energy $E^{cl}(\mathbf{k}_{1/2}) = -2(1 + \alpha)$ a continuum of different ground states exists. This case is discussed in detail in the work of Jolicœur *et al* [11].

(iii) When $\alpha > 1$, the minima move towards the origin of the BZ on straight lines bisecting its faces. Generically, the ground states are incommensurate spiral structures, (4), with energy $E^{cl}(\mathbf{k}) = -3\alpha + 1/\alpha$ in this case. The star of \mathbf{k} consists of six \mathbf{k} vectors which generate three different spiral structures (4). In the limit $\alpha \rightarrow \infty$ the three sublattices decouple and the minima occur at the corners of the BZ of the sublattices.

For our numerical diagonalization of the quantum model (1) we have used the Lanczos method. We have confined our attention to the eigenspace of H with minimal total z -component of the spin. For the 21-site cell this space is spanned by the basis $\{|\mu\rangle\}$ with

$$S_i^z |\mu\rangle = \mp \frac{1}{2} |\mu\rangle \quad i = 1, \dots, 21 \tag{7a}$$

$$\sum_{i=1}^{21} S_i^z |\mu\rangle = \frac{1}{2} |\mu\rangle. \tag{7b}$$

Owing to the translational invariance of H this eigenspace separates into 21 invariant subspaces labelled by the 21 momentum quantum numbers $\mathbf{k}_0, \mathbf{k}_1, -\mathbf{k}_1, \mathbf{k}_2^{(s)}, \mathbf{k}_3^{(s)}, \mathbf{k}_4^{(s)}$, $s = 0, \dots, 5$. The superscript s enumerates the star of vectors obtained from $\mathbf{k}_n^{(0)}$ by counterclockwise C_6 rotations. The location of the five basic \mathbf{k} vectors in the BZ is shown in figure 2. Since H is invariant under C_6 rotations the eigenvalues associated with a star of vectors are degenerate. We shall therefore omit the superscript s in the labelling of the eigenvalues.

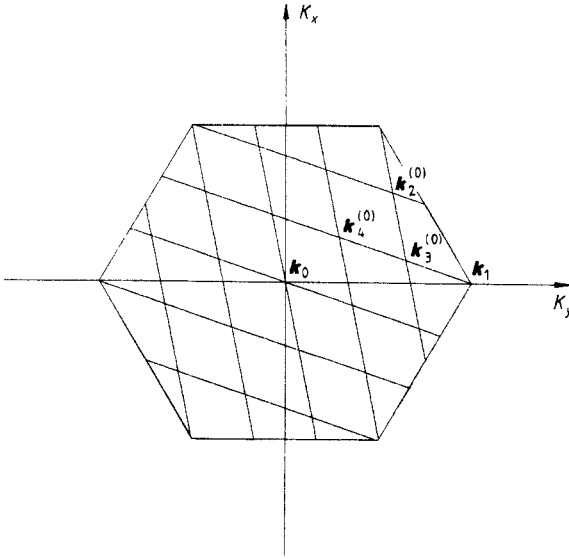


Figure 2. The Brillouin zone associated with the 21-site Marland-Betts cell: $\mathbf{k}_1 = \pi \cdot (4/3, 0)$, $\mathbf{k}_2^{(0)} = \pi \cdot (16/21, 8\sqrt{3}/21)$, $\mathbf{k}_3^{(0)} = \pi \cdot (6/7, 2\sqrt{3}/21)$, $\mathbf{k}_4^{(0)} = \pi \cdot (8/21, 4\sqrt{3}/21)$, $\mathbf{k}_0 = (0, 0)$.

The lowest energy levels $E^{qu}(\mathbf{k}_r)$, $r = 0, \dots, 4$, of H in the momentum subspaces are plotted in figure 3(a) as functions of the NNN interaction α . For $\alpha \gg 1$, the graphs of $E^{qu}(\mathbf{k}_r)$ approach straight lines.

$$E^{qu}(\mathbf{k}_r) \approx 3\alpha E_7^{qu} \quad r = 0, \dots, 4 \tag{8}$$

where $E_7^{qu} = -9$ is the ground-state energy of the decoupled 7-site subsystems of our model. The classical energies $E^{cl}(\mathbf{k}_r) = J(\mathbf{k}_r)$ are shown in figure 3(b). Obviously, there is little resemblance between the behaviour of the classical and the quantum levels. One feature that is shared by them is a crossing of the lowest levels at $\alpha_1^{qu} \approx 0.253$ and at $\alpha_1^{cl} \approx 0.173$ indicating a discontinuous change of symmetry of the ground states. As we have mentioned before, for the infinite system a crossing of the lowest classical energies occurs at $\alpha = \frac{1}{8}$, where the minimum of $J(\mathbf{q})$ at $\mathbf{q} = \mathbf{k}_{1/2}$ begins to develop. This point in \mathbf{k} space is not accessible to the periodic 21-site system. Therefore, instead of $E^{cl}(\mathbf{k}_{1/2})$, $E^{cl}(\mathbf{k}_2)$ becomes the lowest classical level at $\alpha > \alpha_1^{cl}$. By analogy with the classical case one would thus expect the quantum ground state to change from $|\mathbf{k}_1\rangle$ to $|\mathbf{k}_2\rangle$ at α_1^{qu} (we use a self-explanatory notation for the quantum states here). Instead, it changes to $|\mathbf{k}_4\rangle$. Also, the crossing of $E^{cl}(\mathbf{k}_1)$ and $E^{cl}(\mathbf{k}_4)$ at $\alpha_3^{cl} \approx 0.827$ is not matched by a crossing of the corresponding quantum levels for $\alpha > \alpha_1^{qu}$. Because of these differences one might get the impression that the classical approach yields little insight into the behaviour of the finite quantum system under consideration.

In the following we shall consider the structure function $S(\mathbf{k})$ for the ground states $|\mathbf{k}_1\rangle$ and $|\mathbf{k}_4^{(0)}\rangle$ of our 21-site system. In contrast to the impression suggested by the energy levels of our 21-site system we shall find that $S(\mathbf{k})$ reflects the classical picture of the model (1) in various respects. Owing to the translational invariance and the invariance of H under rotations in spin space the general expression for $S(\mathbf{k})$ reduces to

$$S(\mathbf{k}) = 3 \sum_{i=1}^{21} \cos(\mathbf{k} \cdot (\mathbf{R}_0 - \mathbf{R}_i)) g^{zz}(\mathbf{R}_0 - \mathbf{R}_i) \tag{9}$$

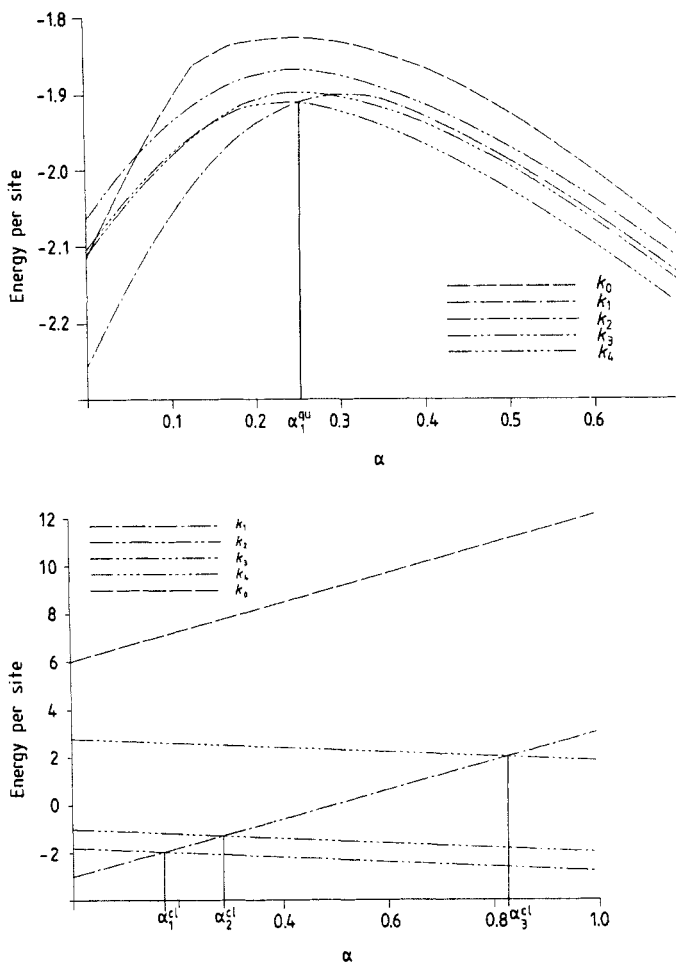


Figure 3. (a) Lowest energy levels $E^{\text{qu}}(k)$ of the 21-site quantum system (1) in the momentum subspaces against α ; $\alpha_1^{\text{qu}} \approx 0.253$. (b) The classical energies $E^{\text{cl}}(k) = 2J(k)$ against α ; $\alpha_1^{\text{cl}} \approx 0.173$, $\alpha_2^{\text{cl}} \approx 0.286$, $0.8\alpha_3^{\text{cl}} \approx 0.827$.

where

$$g^{zz}(\mathbf{R}_0 - \mathbf{R}_i) = \langle \mathbf{k}_{\text{gs}} | S_0^z \cdot S_i^z | \mathbf{k}_{\text{gs}} \rangle \tag{10}$$

with

$$\mathbf{k}_{\text{gs}} = \begin{cases} \mathbf{k}_1 & \text{for } \alpha < \alpha_1^{\text{qu}} \\ \mathbf{k}_4^{(0)} & \text{for } \alpha > \alpha_1^{\text{qu}} \end{cases}$$

are the two spin correlations in the ground states of the 21-sites system. Plots of the $g^{zz}(\mathbf{R})$ as functions of the NNN interaction α are shown in figure 4. The reduction of the sixfold rotational symmetry of the $g^{zz}(\mathbf{R})$ to a twofold reflection symmetry as α increases through α_1^{qu} is in full agreement with the classical picture. In figure 5 the structure function $S(\mathbf{k})$ is displayed at the points \mathbf{k}_0 , \mathbf{k}_1 , $\mathbf{k}_2^{(0)}$, $\mathbf{k}_3^{(0)}$ and $\mathbf{k}_4^{(0)}$ (see figure 3) for several values of α . In the least symmetric case $S(\mathbf{k})$ takes eleven different values in the BZ. The above five points are those members of the stars of \mathbf{k}_1 , \mathbf{k}_2 , \mathbf{k}_3 and \mathbf{k}_4

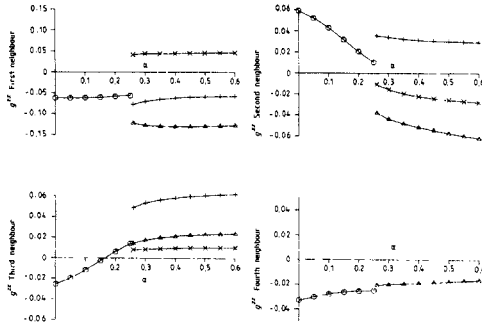


Figure 4. Two-spin correlations $g^{zz}(\mathbf{R}_i - \mathbf{R}_j)$ of first-, second-, third- and fourth-neighbour spins. For $\alpha < \alpha_1^{qu}$ the two-spin correlations are independent of the lattice direction, for $\alpha > \alpha_1^{qu}$ they differ in the three lattice directions. Note that there are only two fourth neighbours.

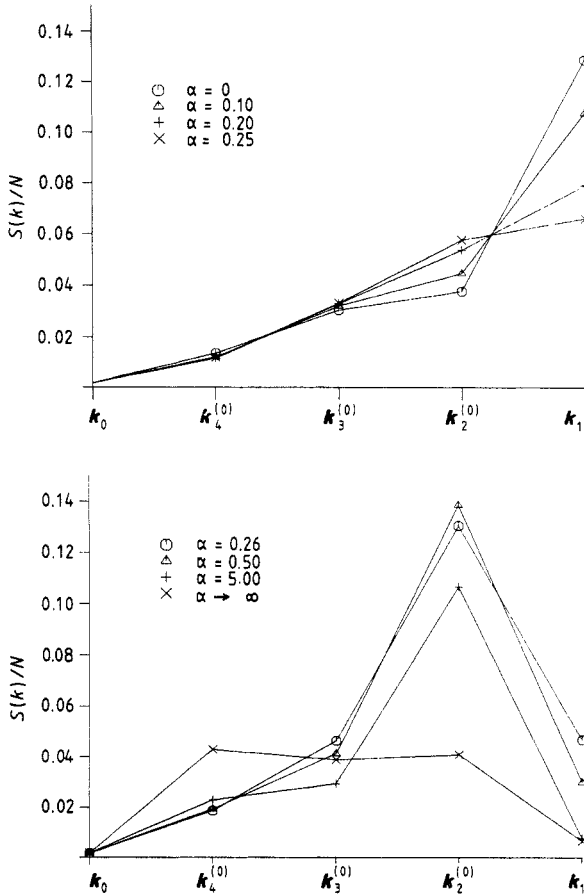


Figure 5. The structure function $S(\mathbf{k})$ at five points of the Brillouin zone for various NNN couplings α (a) $\alpha < \alpha_1^{qu}$; (b) $\alpha > \alpha_1^{qu}$. The data points for $\alpha \rightarrow \infty$ were obtained by setting the NN coupling equal to zero.

that lie closest to the loci of the minima of $J(\mathbf{k})$ which represent the ground-state energies of the infinite classical system. In the classical approach $S(\mathbf{k})$ consists of a single spike of height $3N$ which is located at \mathbf{k}_1 for $\alpha < \alpha_1^{\text{cl}}$ and which jumps to $\mathbf{k}_2^{(0)}$ for the 21-site system as α grows through α_1^{cl} . In the quantum case $S(\mathbf{k})$ is spread out over the entire BZ, but, as is seen in figure 5, the locus of its maximum jumps from \mathbf{k}_1 to $\mathbf{k}_2^{(0)}$ as α increases through α_1^{qu} in full agreement with the classical picture.

We have also found a remarkable connection between the structure function $S(\mathbf{k})$ and the energies $E^{\text{cl}}(\mathbf{k})$ shown in figure 3(b). To illustrate this connection we display in figure 6 the values of $S(\mathbf{k})$ for the same set of \mathbf{k} vectors as in figure 5 as functions of α . One sees that while the inequalities

$$S(\mathbf{k}_2^{(0)}) > S(\mathbf{k}_3^{(0)}) > S(\mathbf{k}_4^{(0)}) > S(\mathbf{k}_0)$$

hold for any finite α , $S(\mathbf{k}_1)$ jumps across $S(\mathbf{k}_2)$ at α_1^{qu} and crosses $S(\mathbf{k}_3)$ and $S(\mathbf{k}_4)$ at $\alpha_2^{\text{qu}} \approx 0.266$ and at $\alpha_3^{\text{qu}} \approx 0.95$ respectively. Although the crossings of the $S(\mathbf{k})$ and of the $E^{\text{cl}}(\mathbf{k})$ do not occur at identical values of α and despite of the discontinuities in $S(\mathbf{k})$ there is an obvious relation between the two quantities: in large intervals of the α axis the values of the structure function shown in figure 6 are ordered in the same way as for a classical thermal ensemble, i.e. $S(\mathbf{k}_\mu) < S(\mathbf{k}_\nu)$ if $E^{\text{cl}}(\mathbf{k}_\mu) > E^{\text{cl}}(\mathbf{k}_\nu)$. Relations of this kind cannot of course, hold for all points of the BZ as there are only five distinct $E^{\text{cl}}(\mathbf{k})$ while generically $S(\mathbf{k})$ takes eleven different values in the BZ. Nevertheless, we consider the above relations significant, since they apply for those points of the BZ of the infinite system, figure 2, that lie closest to the loci of the classical ground states of the infinite system.

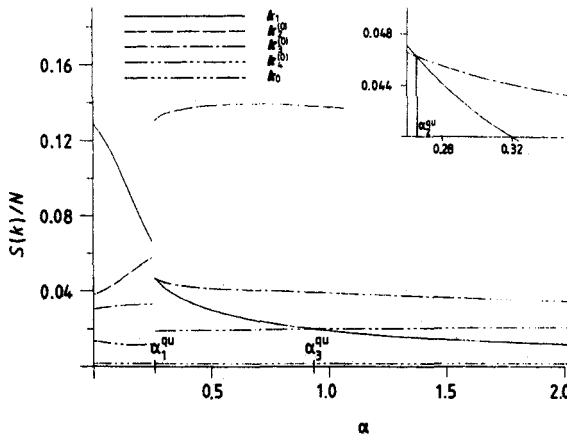


Figure 6. Variation of $S(\mathbf{k})$ with the NNN coupling α for the same \mathbf{k} vectors as in figure 5. The inset shows the crossing of $S(\mathbf{k}_1)$ and $S(\mathbf{k}_3^{(0)})$ at α_2^{qu} .

According to Baskaran [8] chiral symmetry breaking may be expected for the model under consideration when the NNN coupling exceeds a critical value. For a ground state with uniform or staggered long-range chiral order the appropriate order parameters are [9]

$$P_{\mp} = \langle C_{\mp}^+ \cdot C_{\mp} \rangle / N \tag{11}$$

where

$$C_{\mp} = \sum_{i_x, i_y} [\mathbf{S}_{i_1} \cdot (\mathbf{S}_{i_2} \times \mathbf{S}_{i_3}) \mp \mathbf{S}_{i_1} \cdot (\mathbf{S}_{i_3} \times \mathbf{S}_{i_4})]. \tag{12}$$

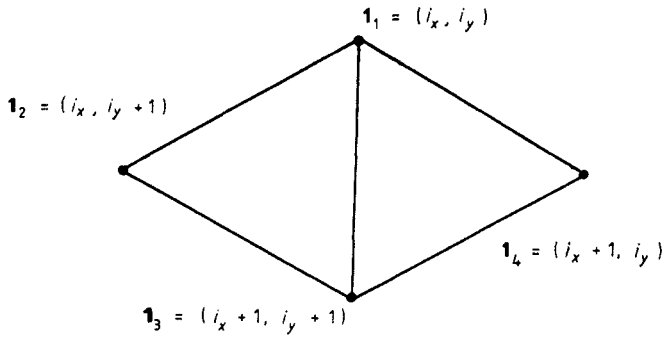


Figure 7. Adjacent elementary plaquettes used in defining the order parameters P_{\mp} .

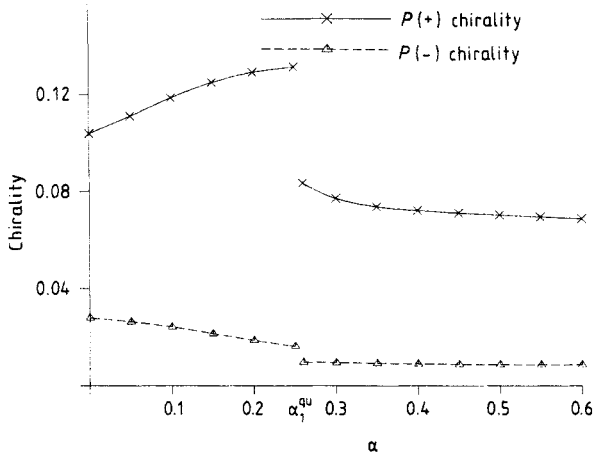


Figure 8. The chiral order parameter P_{\mp} against α .

Here, the sum extends over all pairs of adjacent elementary plaquettes of the lattice, figure 7. The results for our 21-site system displayed in figure 8 reflect the discontinuous change of the symmetry of the ground states, but no significant increase of P_+ with α is observed in either of the two states. Thus our results are not indicative of a state with broken chiral symmetry.

To summarize, our numerical study of the 21-site triangular Heisenberg antiferromagnet with NNN interaction has revealed rather close connections between the quantum and the classical description of this model. In particular, the change in the symmetry of the classical ground state with increasing strength of the NNN interaction is clearly reflected by the behaviour of the structure function. We could not find an indication of chiral symmetry breaking in the ground states of our finite system.

The numerical calculations were carried out at the Regionales Rechenzentrum Niedersachsen, Hannover.

References

- [1] Anderson P W 1987 *Science* **235** 1196
Anderson P W, Baskaran G, Zou Z and Hsu T 1989 *Phys. Rev. Lett.* **58**

- [2] Fazekas P and Anderson P W 1974 *Phil. Mag.* **30** 423
Anderson P W 1983 *Mat. Res. Bull.* **8** 153
Nishimori H and Nakanishi H 1988 *J. Phys. Soc. Japan* **57** 626
Nishimori H and Miyashita S 1986 *J. Phys. Soc. Japan* **55** 4450
- [3] Reger J D and Young A P 1988 *Phys. Rev. B* **37** 5978
Miyashita S 1988 *J. Phys. Soc. Japan* **57** 1934
- [4] Dagotto E and Moreo A 1989 *Phys. Rev. B* **39** 4744
Figueido F, Karlhede A, Kivelson S, Sondhi S, Rocek M and Rokhsar D S 1990 *Phys. Rev. B* **41** 4619
- [5] Huse D A and Elser V 1988 *Phys. Rev. Lett.* **24** 2531
Jolicœur Th and Le Guillou J C 1989 *Phys. Rev. B* **40** 2727
- [6] Klein D J 1982 *J. Phys. A: Math. Gen.* **15** 661
- [7] Kalmeyer V and Laughlin R B 1989 *Phys. Rev. B* **39** 11879
- [8] Baskaran G 1989 *Phys. Rev. Lett.* **63** 2524
- [9] Imada M 1989 *J. Phys. Soc. Japan* **58** 2650
- [10] Marland L R and Betts D D 1980 *Phys. Lett.* **76A** 271
- [11] Jolicœur Th, Dagotto E, Gagliano E and Bacci S 1990 *Preprint Saclay*
- [12] Villain J 1959 *J. Phys. Chem. Solids* **11** 303
Yoshimori A 1959 *J. Phys. Soc. Japan* **14** 807
- [13] Villain J 1977 *J. Physique* **38** 385